J. Phycol. **32**, 799–812 (1996)

MICROENVIRONMENTAL CONTROL OF PHOTOSYNTHESIS AND PHOTOSYNTHESIS-COUPLED RESPIRATION IN AN EPILITHIC CYANOBACTERIAL BIOFILM[1]

Michael Kühl,[2] *Ronnie Nøhr Glud, Helle Ploug, and Niels Birger Ramsing*

Department of Microbial Ecology, Institute of Biological Sciences, University of Aarhus, Ny Munkegade Building 540, DK-8000 Aarhus C, Denmark

ABSTRACT

The photosynthetic performance of an epilithic cyanobacterial biofilm was studied in relation to the in situ *light field by the use of combined microsensor measurements of O_2, photosynthesis, and spectral scalar irradiance. The high density of the dominant filamentous cyanobacteria (*Oscillatoria *sp.) embedded in a matrix of exopolymers and bacteria resulted in a photic zone of <0.7 mm. At the biofilm surface, the prevailing irradiance and spectral composition were significantly different from the incident light. Multiple scattering led to an intensity maximum for photic light (400–700 nm) of ca. 120% of incident quantum irradiance at the biofilm surface. At the bottom of the euphotic zone in the biofilm, light was attenuated strongly to <5–10% of the incident surface irradiance. Strong spectral signals from chlorophyll* a *(440 and 675 nm) and phycobilins (phycoerythrin 540–570 nm, phycocyanin 615–625 nm) were observed as distinct maxima in the scalar irradiance attenuation spectra in the upper 0.0–0.5 mm of the biofilm. The action spectrum for photosynthesis in the cyanobacterial layer revealed peak photosynthetic activity at absorption wavelengths of phycobilins, whereas only low photosynthesis rates were induced by light absorption of carotenoids (450–550 nm).*

Respiration rates in light- and dark-incubated biofilms were determined using simple flux calculations on measured O_2 concentration profiles and photosynthetic rates. A significantly higher areal O_2 consumption was found in illuminated biofilms than in dark-incubated biofilms. Although photorespiration accounted for part of the increase, the enhanced areal O_2 consumption of illuminated biofilms could also be ascribed to a deeper oxygen penetration in light as well as an enhanced volumetric O_2 respiration in and below the photic zone. Gross photosynthesis was largely unaffected by increasing flow velocities, whereas the O_2 flux out of the photic zone, that is, net photosynthesis, increased with flow velocity. Consequently, the amount of produced O_2 consumed within the biofilm decreased with increasing flow velocity. Our data indicated a close coupling of photosynthesis and respiration in biofilms, where the dissolved inorganic carbon requirement of the photosynthetic population may largely be covered by the respiration of closely associated populations of heterotrophic bacteria consuming a significant part of the photosynthetically produced oxygen and organic carbon.

Key index words: action spectra; biofilms; cyanobacteria; diffusion; flow; light penetration; microsensor; Oscillatoria *sp.; photosynthesis*

Epilithic biofilms growing on stones (e.g. in stream beds or trickling filters) are ideal model systems for studies of the interaction and regulation of many microbial processes in periphyton communities such as photosynthesis (Kuenen et al. 1986, Carlton and Wetzel 1987, Dodds 1989a, Glud et al. 1992), denitrification (Nielsen et al. 1990, Dalsgaard and Revsbech 1992), and oxygen respiration and sulfate reduction (Kühl and Jørgensen 1992a, Ramsing et al. 1993). Photosynthetic biofilms are densely populated microbial communities with a complex microstructure that are characterized by steep chemical gradients and a very strong attenuation of light within a photic zone ranging from <0.5 mm to a few millimeters in thickness. Studies of microbenthic photosynthesis require experimental techniques with a high spatial resolution and sensitivity. A light–dark shift technique for determining the depth distribution of oxygenic photosynthesis at a spatial resolution of <100 μm using oxygen microelectrodes has been developed by Revsbech and Jørgensen (1983). With this technique it is possible to measure gross photosynthesis independent of respiration. This is a major advantage of the microelectrode technique over the traditionally used gas exchange or ^{14}C-isotope methods, which are difficult to apply because of the close coupling of photoautotrophic and heterotrophic processes in microbenthic environments (Revsbech et al. 1981, Lindeboom et al. 1985). The gross photosynthesis measured by the O_2 microelectrode light–dark shift technique includes O_2 that is consumed via photorespiration but does not include oxygen consumed by pseudocyclic electron transport (Mehler reaction) (Glud et al. 1992).

Photosynthetic microorganisms in sediments and biofilms live in a diffuse light field where they receive a major part of the light for photosynthesis as scattered light (Jørgensen and Des Marais 1988, Kühl and Jørgensen 1994, Kühl et al. 1994b). It is therefore important to relate the measured photosynthesis rate to the actual light field around the photosynthetic microorganisms to understand the regulation and dynamics of microbenthic photosynthesis. The use of a fiber-optic microprobe with a terminal light diffusion sphere allows direct measurements of

[1] Received 27 December 1995. Accepted 3 June 1996.

[2] Present address and address for reprint requests: Max-Planck-Institute for Marine Microbiology, Microsensor Research Group, Celsiusstr. 1, D-28359 Bremen, Germany.

scalar irradiance, that is, the total quantum flux from all directions incident at a point (Lassen et al. 1992a). Scalar irradiance is the most relevant optical parameter in relation to microbenthic photosynthesis, as it integrates light from all directions and thus includes scattered light, which is of paramount importance in biofilms and sediments (Jørgensen and Des Marais 1988, Kühl and Jørgensen 1994, Kühl et al. 1994b). By the combined use of O_2 microelectrodes and fiber-optic scalar irradiance microprobes, the photosynthetic performance of phototrophs can be related to their *in situ* light field in microbenthic communities (Kühl and Jørgensen 1992b, Lassen et al. 1992b, Ploug et al. 1993). Only a few studies of photosynthetic biofilms have incorporated direct measurements of the chemical and physical microenvironment within the biofilm. Most of these studies related photosynthesis to incident irradiance (e.g. Sand-Jensen et al. 1985, Kuenen et al. 1986, Carlton and Wetzel 1987, Sand-Jensen and Revsbech 1987, Jensen and Revsbech 1989) or underestimated total irradiance by using fiber-optic microprobes with either a narrow acceptance angle or nonideal light-collecting properties (Dodds 1989a, 1992, Williams and Carpenter 1990).

Another important regulating factor for microbial processes in natural biofilms is the presence of a diffusive boundary layer (DBL). The DBL acts as a diffusion barrier for exchange of solutes between the biofilm and the overlaying turbulent water (Jørgensen and Revsbech 1985, Jørgensen 1994), and the DBL thickness is dependent on flow. High flow velocities lead to a thinner DBL and thus increased solute exchange across the biofilm–water interphase, which again affects the chemical gradients and the microbial activity within the biofilm (Jørgensen and Revsbech 1985, Jørgensen and Des Marais 1990).

The close coupling of photosynthesis and respiratory processes in biofilms makes it likely that the regulation of photosynthesis by light and flow also affects the respiration within illuminated biofilms (Kuenen et al. 1986). A concurrent increase of photosynthesis and O_2 respiration with increasing irradiance has been demonstrated in artificially grown biofilms (Jensen and Revsbech 1989). Dodds (1989b) found an increase of the photosynthetic rate with flow velocity over epilithic colonies of the cyanobacterium *Nostoc parmelioides*. Effects of light and flow velocity on photosynthesis and photosynthesis-coupled respiration remain, however, virtually unstudied in natural biofilms (Neely and Wetzel 1995).

In this study, we used O_2 microelectrodes and fiber-optic microprobes for scalar irradiance to quantify the photosynthetic performance of an epilithic cyanobacterial biofilm. The photosynthetic performance was related to the microstructure of the biofilm by scanning electron microscopy (SEM). The regulatory aspects of light and water flow on photosynthesis and photosynthesis-coupled respiration in biofilms were investigated. The experiments were done under controlled laboratory conditions and our results therefore demonstrate the principles of microbial regulation rather than *in situ* conditions. A detailed methodological study of the oxygen microelectrode technique for photosynthesis measurements and the importance of photorespiration was done in the same type of biofilm by Glud et al. (1992).

MATERIALS AND METHODS

Biofilms growing on stones were sampled from the light-exposed surface of a trickling filter at Skødstrup Sewage Treatment Plant, Skødstrup, Denmark. The biofilms were 3–5 mm thick with a smooth blue-green surface layer of cyanobacteria and consisted of a dense matrix of bacteria and exopolymers (Fig. 1). Throughout the biofilm, large numbers of sludgeworms (*Tubifex* sp.) and dipteran larvae (*Psycoda* sp.) were found. After sampling, biofilm was removed from most of the stone, leaving a small homogeneous biofilm area of 1–3 cm^2. Most larger worms and larvae were then carefully removed with forceps. The rinsed biofilm area left on the stone either was used directly for measurements or was carefully removed and transferred to a small black Petri dish with semisolid agar (1.5% at 35°–40° C). The agar soldered to the bottom of the biofilm and partially embedded the biofilm, leaving the upper surface free of agar. When the agar cooled down the biofilm sample was thus fixed in the Petri dish, which was subsequently immersed in aerated tap water at room temperature prior to measurements in the laboratory.

The experiments were done at room temperature (20°–22° C). The biofilm sample was positioned in an aquarium with ca. a 1-cm-thick layer of aerated tap water flowing continuously over the biofilm surface. Water movement was created by directing a gentle air stream over the water surface via a Pasteur pipette connected to an air pump. Flow velocity was estimated by following small suspended particles in the water 3–5 mm above the biofilm through a dissection microscope. By controlling the air pump with a variotransformer, it was possible to adjust the flow velocity to known values. The microsensors were mounted on a motor-driven micromanipulator (Märtzhäuser, Germany), which was interfaced to a desktop computer and controlled by a Pascal program. Surface positioning of the microsensors was done visually through a dissection microscope.

Biofilm microstructure. The microstructure of the biofilm was studied by SEM on 3–5-mm-thick vertical sections of biofilm. Blocks of fresh biofilm were cut and placed on filter paper with the vertical cut facing upward. The samples were imbedded in a viscous matrix (OCT, Tissue-Tek II; Miles, Elkhart, Indiana) and were frozen rapidly by placing the filter on a metal plate in contact with liquid nitrogen. Direct immersion in liquid nitrogen resulted in freeze fractures of the biofilm samples and was therefore avoided. Prior to fixation and dehydration, the samples were kept at −80° C. The OCT cover of the biofilm was removed with a razor blade while the sample was still frozen. The exposed biofilm samples were then fixed and dehydrated by critical point sublimation (Paerl and Shimp 1973), covered by Pt-sputtering, and observed through a Zeiss scanning electron microscope.

Oxygen measurements. Depth profiles of oxygen (dissolved O_2) concentration were measured by a Clark-type oxygen microelectrode with a guard cathode (Revsbech 1989) connected to a picoammeter and a stripchart recorder. The electrodes had a tip diameter of 2–10 μm, a stirring sensitivity of 1–2%, and a 90% response time of 0.2–0.4 s. Linear calibration of electrodes was done from electrode readings in air-saturated water above the biofilm and in the anoxic part of the biofilm.

Oxygenic photosynthesis. Gross photosynthesis at depth z, P(z),

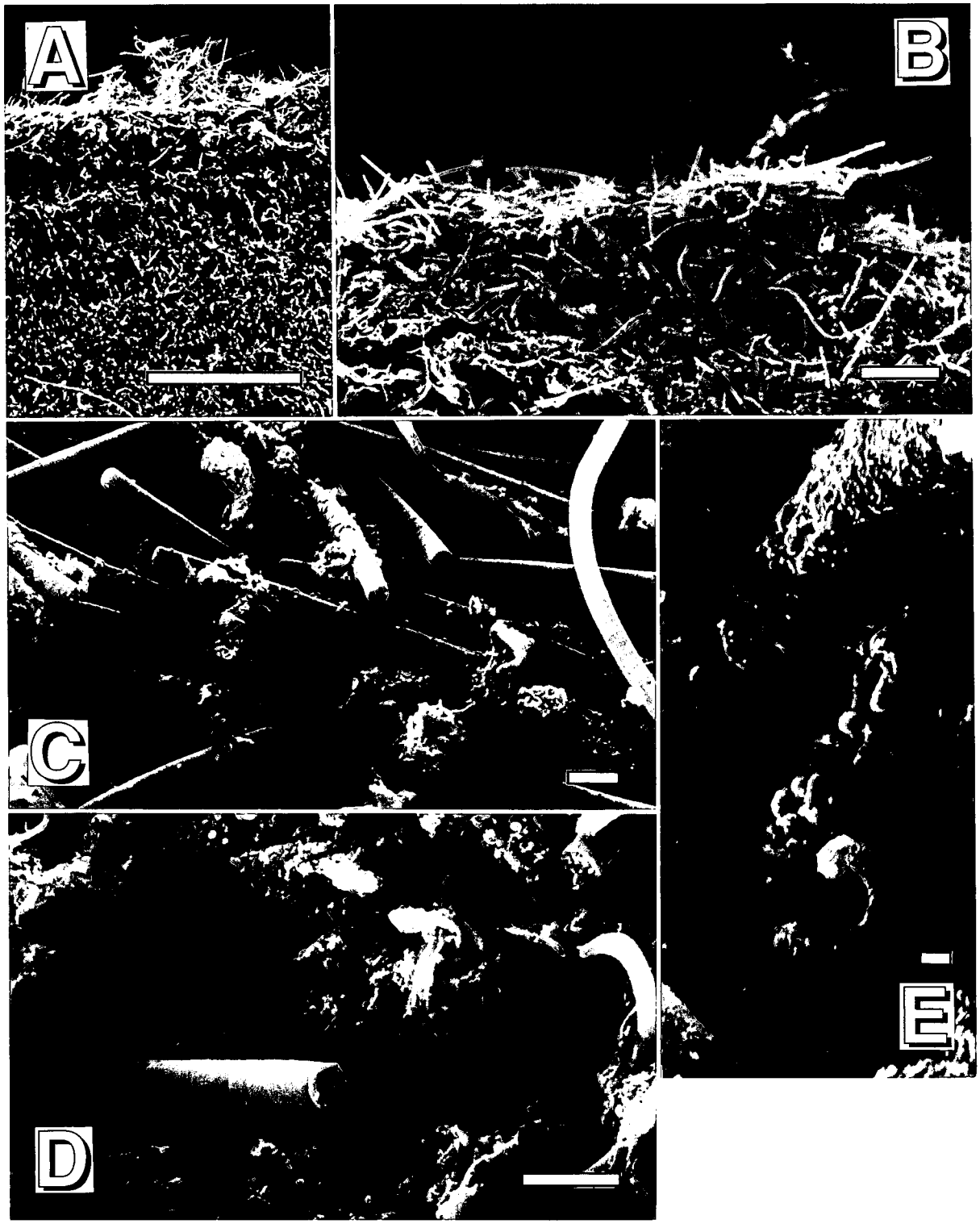

FIG. 1. Scanning electron micrographs. A, B) 400–700-μm-thick surface layer of filamentous cyanobacteria (*Oscillatoria* sp.) in an epilithic biofilm. C–E). Dense matrix of exopolymers and bacteria surrounding the cyanobacteria. Scale bars = 1 mm (A), 100 μm (B), 10 μm (C, D), 1 μm (E).

was determined with the microelectrode light–dark shift technique in units of nmol $O_2 \cdot cm^{-3}$ biofilm $\cdot s^{-1}$ (Revsbech and Jørgensen 1983, Glud et al. 1992). The principle of the method is outlined in Figure 2C. The gross rate of photosynthesis is estimated as the initial decrease of oxygen at a specific depth during the first 1–2 s after eclipse of the light source, assuming 1) a steady-state O_2 distribution before darkening, 2) an identical O_2 consumption before and during the darkening period, and 3)

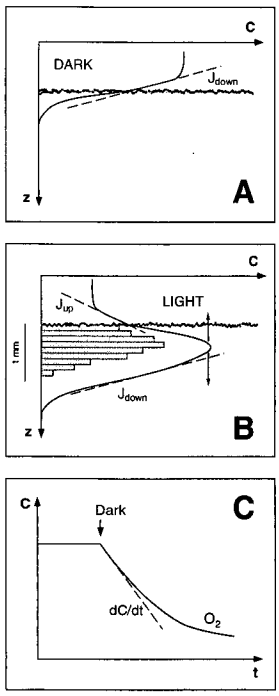

OXYGEN FLUX CALCULATIONS

DARK: $R_{dark} = J_{down} = -D_0 \frac{dC(z)}{dz}$

LIGHT: $P_n = J_{up} = -D_0 \frac{dC(z)}{dz}$

$J_{down} = -\Phi D_s \frac{dC(z)}{dz}$

$P_{n,phot} = |J_{up}| + |J_{down}|$

$R_{light} = P_g - P_n$

$R_{phot} = P_g - P_{n,phot}$

OXYGEN MICROELECTRODE LIGHT-DARK SHIFT METHOD

LIGHT: $\frac{dC(z)}{dt} = D_s \frac{d^2C(z)}{dz^2} + P(z) - R(z)$

At steady state:

$\frac{dC(z)}{dt} = 0 \Leftrightarrow P(z) = R(z) - D_s \frac{d^2C(z)}{dz^2}$

After darkening:

$\frac{dC(z)}{dt} = -\left[R(z) - D_s \frac{d^2C(z)}{dz^2}\right]$

thus:

$P(z) = -\frac{dC(z)}{dt}$

FIG. 2. Flux calculations on steady-state O_2 concentration profiles and the light–dark shift method for measuring oxygenic photosynthesis in microbenthic communities with oxygen microelectrodes. Lines represent O_2 concentration, and bars represent gross photosynthesis. A) Calculation of areal dark respiration. B) Calculation of areal net photosynthesis and respiration in illuminated biofilms. C) Theory behind the light–dark shift method. Flux calculations are done at steady state using Fick's first law for one-dimensional diffusion. Light–dark shift measurements are based on non-steady-state O_2 measurements using a diffusion-reaction model based on Fick's second law of diffusion. Partly redrawn after Karsten and Kühl (1996).

identical diffusive fluxes at that depth during the measurement. These assumptions have been evaluated and confirmed in an earlier study of the same biofilms, where a detailed discussion of the light–dark shift method is presented (Glud et al. 1992). That study indicated that gross photosynthesis determined by O_2 microelectrodes in this way includes oxygen consumed by photorespiration but not by the Mehler reaction. Areal gross photosynthesis, P_g, was calculated by integrating the photosynthesis profiles over depth. An overview of significant symbols and abbreviations used throughout this paper can be found in Table 1.

Flux calculations of net photosynthesis and respiration. Diffusive fluxes of oxygen, J, were calculated from steady-state O_2 profiles by Fick's first law of one-dimensional diffusion:

$$J = D_e \frac{dC(z)}{dz}, \quad (1)$$

where D_e is the effective diffusion coefficient and dC/dz is the concentration gradient. Note that $D_e = \phi D_s$, that is, the product of porosity, ϕ, and the apparent diffusion coefficient, D_s, in the biofilm.

The dark respiration of the biofilm, R_{dark}, was estimated as the flux of O_2 into the biofilm calculated from Eq. (1) by using the linear O_2 gradient in the DBL above the biofilm (cf. Jørgensen and Revsbech 1985) (Fig. 2A). Similarly, the net photosynthesis of the biofilm, P_n, was calculated as the diffusive flux of O_2 into the overlaying water across the DBL in the light (Fig. 2B). For the flux calculations in the DBL, a molecular diffusion coefficient of O_2 in freshwater, $D_0 = D_e = 2.06\ 10^{-5}\ cm^2 \cdot s^{-1}$ (calculated for 20° C from Broecker and Peng 1974), was used. The areal respiration of the biofilm in the light, R_{light}, was calculated as the difference between total gross and net photosynthesis, $P_g - P_n$. Note that R_{light} is the sum of biofilm respiration within and below the photic zone.

Net photosynthesis and respiration were also calculated for the photic zone alone (Jensen and Revsbech 1989, Glud et al. 1992). The areal net photosynthesis of the photic zone, $P_{n,phot}$, was calculated as the sum of the flux of O_2 into the overlaying water across the DBL, J_{up}, and the flux into the biofilm below the photic zone, J_{down} (Fig. 2B). The downward flux was calculated from the slope of the O_2 profile at the lower boundary of the photic zone using Eq. (1) with a D_e value of $1.41\ 10^{-5}\ cm^2 \cdot s^{-1}$. This average value of D_e was determined for the biofilm in an earlier study (Glud et al. 1995). The areal respiration of the photic zone in light was then calculated as $R_{phot} = P_g - P_{n,phot}$.

Average volumetric rates of O_2 respiration (in units of nmol $O_2 \cdot cm^{-3}$ biofilm $\cdot s^{-1}$) of distinct zones of biofilm were calculated by dividing areal respiration rates determined from the flux calculations with the depth of the reaction zone, that is, the depth of the photic zone or the O_2 penetration depth, assuming a constant D_e throughout the biofilm.

Light measurements. Total irradiance was quantified by direct measurements of spectral scalar irradiance (400–880 nm) with a fiber-optic microprobe coupled to a sensitive diode array detector system (Kühl and Jørgensen 1992b). The fiber-optic microprobe consisted of a small diffusing sphere of ~80 μm diameter cast on the flat cut tip of a tapered optical fiber that was coated with black enamel paint to prevent light from entering on the tapered sides (Lassen et al. 1992a, Kühl et al. 1994b). The diffusing sphere resulted in an isotropic (±10%) response to incident light, and the fiber-optic microprobe thus measured scalar irradiance, that is, the spherically integrated quantum flux from all directions about a point.

Photosynthetic available light (PAR), that is, integrated scalar irradiance from 400 to 700 nm, E_0(PAR), was calculated from

TABLE 1. *Definition of abbreviations.*

C(z)	Oxygen concentration at depth z ($\mu mol \cdot L^{-1}$)
D_0	Oxygen diffusion coefficient in water ($cm^2 \cdot s^{-1}$)
D_e	Effective oxygen diffusion coefficient in biofilm ($cm^2 \cdot s^{-1}$)
E_0	Photon scalar irradiance ($\mu mol\ photons \cdot m^{-2} \cdot s^{-1}$)
E_d	Incident downwelling photon irradiance ($\mu mol\ photons \cdot m^{-2} \cdot s^{-1}$)
J	Oxygen flux ($nmol\ O_2 \cdot cm^{-2} \cdot s^{-1}$)
K_0	Attenuation coefficient of scalar irradiance (mm^{-1})
P(z)	Volumetric gross photosynthesis at depth z ($nmol\ O_2 \cdot cm^{-3} \cdot s^{-1}$)
P_g	Gross areal photosynthesis of biofilm ($nmol\ O_2 \cdot cm^{-2} \cdot s^{-1}$)
P_n	Net areal photosynthesis of biofilm ($nmol\ O_2 \cdot cm^{-2} \cdot s^{-1}$)
$P_{n,phot}$	Net areal photosynthesis of the photic zone ($nmol\ O_2 \cdot cm^{-2} \cdot s^{-1}$)
R(z)	Volumetric oxygen respiration at depth z ($nmol\ O_2 \cdot cm^{-3} \cdot s^{-1}$)
R_{dark}	Areal biofilm respiration in dark ($nmol\ O_2 \cdot cm^{-2} \cdot s^{-1}$)
R_{light}	Areal biofilm respiration in light ($nmol\ O_2 \cdot cm^{-2} \cdot s^{-1}$)
R_{phot}	Areal respiration of the photic zone in light ($nmol\ O_2 \cdot cm^{-2} \cdot s^{-1}$)

scalar irradiance spectra corrected for the spectral sensitivity of the detector system and related to the incident downwelling irradiance measured with a photon irradiance meter (LiCor LI-185, LI-192) (more details in Kühl and Jørgensen 1992b and Lassen et al. 1992a, b). Attenuation spectra of scalar irradiance, $K_{0,\lambda}$, were calculated as $K_{0,\lambda} = \ln(E_{1,\lambda}/E_{2,\lambda})/(z_2 - z_1)$, where $E_{1,\lambda}$ and $E_{2,\lambda}$ are the scalar irradiance spectra at depth z_1 and z_2, respectively (Kühl and Jørgensen 1994).

Photosynthesis vs. irradiance curves and action spectra. Combined measurements of scalar irradiance and photosynthesis were done with oxygen and scalar irradiance microsensors mounted on the same micromanipulator with the sensor tips positioned <100 μm apart in the same horizontal plane. The sensors were tilted at a zenith angle of 135° relative to the vertically incident light. Photosynthesis as a function of light intensity (photosynthesis vs. irradiance [P vs. I] curves) was measured by illuminating the biofilm with collimated light from a fiber-optic tungsten-halogen lamp (150 W, Schott KL1500). Different irradiances were created by inserting neutral density filters in the light path. For most experiments, the fiber-optic light source was equipped with a heat filter that cut off infrared light. Even without a conversion filter the heating of samples was minimal due to the fact that irradiances maximally reached ca. 200–250 μmol photons·m^{-2}·s^{-1} in all experiments.

Action spectra of photosynthesis in the upper 0.1 mm of the biofilm were determined at 10-nm intervals from 410 to 700 nm as described by Ploug et al. (1993). The actinic monochromatic light (HBW 10 nm) came from a 75-W Xe lamp coupled to a monochromator (Oriel Corp.). The incident irradiance of monochromatic light was 10–15 μmol photons·m^{-2}·s^{-1}. The biofilm was also illuminated with background light from a fiber-optic halogen lamp (Schott KL1500) equipped with a 600-nm (HBW 30 nm) bandpass filter to ensure excitation of photosystem II at all actinic wavelengths. Background irradiance was also 10–15 μmol photons·m^{-2}·s^{-1}. The combined light intensity was, however, low enough to avoid saturation of photosynthesis at all wavelengths from 400 to 700 nm. Correction for changes in the photosynthetic activity due to movement of the cyanobacteria and so forth during the recording of the action spectrum was done by making reference measurements at 480 nm after every third measurement throughout the spectrum.

RESULTS

Biofilm microstructure and migration. Light microscopy and SEM of the biofilm revealed the presence of a ca. 0.5–1-mm-thick surface layer of motile filamentous cyanobacteria (*Oscillatoria* sp.) that formed a dense network of filaments embedded in an exopolymer matrix (Fig. 1A, B). Highest densities of the cyanobacteria were always found in the upper 0.5 mm of the biofilm. A high density of bacteria was found in the exopolymer matrix, and we frequently observed bacteria closely associated with the cyanobacterial filaments (Fig. 1C–E). The bulk (2–5 mm) of the biofilm below the surface layer of cyanobacteria was composed of a dense matrix of mainly unicellular bacteria and exopolymers.

The smooth surface layer of cyanobacteria (Fig. 1A, B) resulted in a relatively low horizontal heterogeneity within the biofilm at moderate irradiances. Multiple microsensor measurements of O_2 profiles done at random within an area of ca. 1 cm^2 were consequently very similar with a relative standard deviation of <25% (data not shown). The surface structure of the biofilm changed due to lateral migration of the cyanobacterial filaments into dense tufts at the highest investigated irradiances (150–200 μmol photons·m^{-2}·s^{-1}). The maximum irradiance at the sampling site in the summer is around 1000–1500 μmol photons·m^{-2}·s^{-1}, whereas an ordinary cloudy day in Denmark would correspond to ca. 100–200 μmol photons·m^{-2}·s^{-1}. Besides changing the local density of cyanobacteria, this aggregation into tufts at high irradiances increased the roughness of the biofilm, and the DBL thickness thus increased from 250 to 400 μm between tufts (compare e.g. O_2 profiles in Figs. 3 and 4).

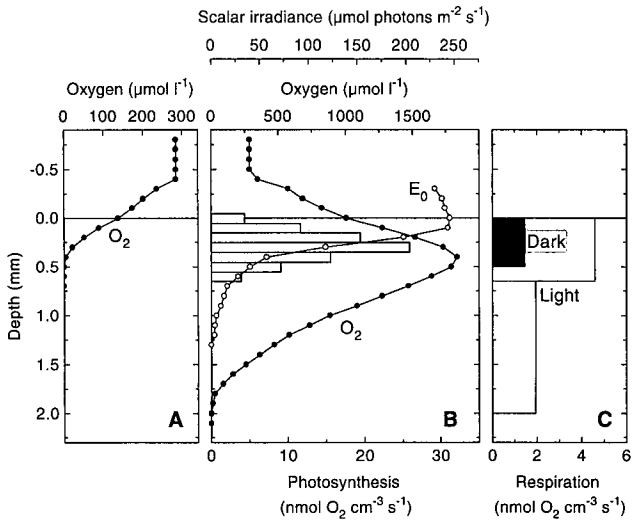

FIG. 3. O_2, photosynthesis, and light distribution in a cyanobacterial biofilm. A) Steady-state O_2 profiles in dark-incubated biofilm. B) Steady-state depths profiles of O_2, gross photosynthesis (shaded bars), and photon scalar irradiance, E_0, in illuminated biofilm. C) Depth distribution of volumetric O_2 respiration in dark-incubated (black box) and illuminated biofilm (shaded boxes). Incident photon irradiance at the biofilm surface was 200 μmol photons·m^{-2}·s^{-1}.

At high irradiances the variability of the measured microprofiles increased. Formation and release of O_2 bubbles from the biofilm started at an incident irradiance of ca. 100 μmol photons·m^{-2}·s^{-1}, and it was not possible to measure steady-state microprofiles at higher irradiances than 200–250 μmol photons·m^{-2}·s^{-1} when intense bubble formation started to disrupt a significant part of the biofilm surface. Photosynthetic rate measurements at different horizontal positions generally exhibited a higher variability than the oxygen depth profiles (see e.g. Fig. 4).

Steady-state profiles of oxygen, photosynthesis, and light. The high heterotrophic activity of the biofilm resulted in an oxygen penetration depth of only 0.2–0.5 mm in the dark (Fig. 3A). However, when the biofilm was illuminated, photosynthesis in the dense cyanobacterial surface layer increased the O_2 concentration within the biofilm, and at an incident irradiance of ca. 17.5 μmol photons·m^{-2}·s^{-1} the biofilm reached the oxygen compensation point, where

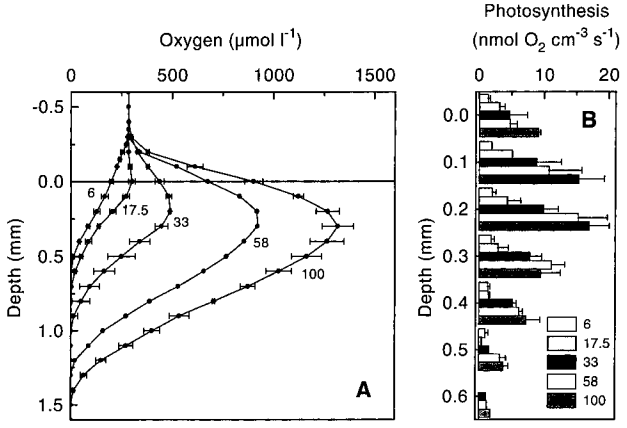

FIG. 4. Steady-state depth profiles of A) O_2 concentration and B) gross photosynthesis measured at different irradiances. Numbers on graph indicate the incident photon irradiance at the biofilm surface. Data points represent the mean of one to three measurements, and the error bars indicate the standard deviation.

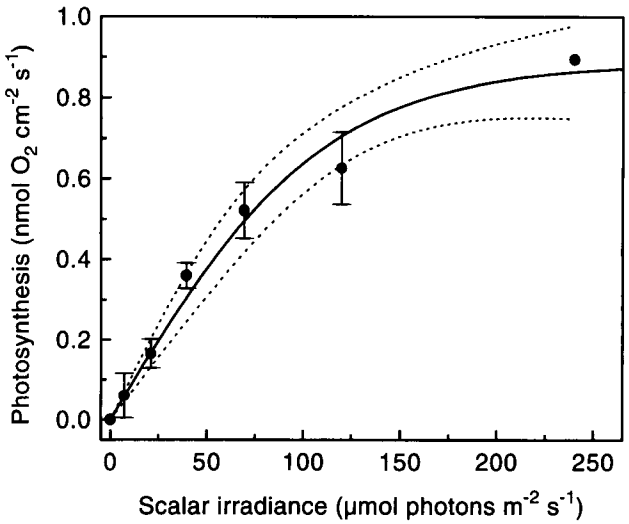

FIG. 5. Gross areal photosynthesis of the biofilm vs. photon scalar irradiance at the biofilm surface. Data points represent the mean of one to three measurements, and error bars indicate the standard deviation. The solid line was obtained by fitting a hyperbolic tangent function (Jasby and Platt 1976) to the data ($r^2 = 0.983$, $\chi^2 = 0.002$). Dotted lines indicate the 95% confidence interval of the fit. Curve fitting was done with a nonlinear regression Levenberg-Marquardt algorithm (Origin 3.0, MicroCal Software Inc.).

photosynthetic O_2 production balanced the O_2 consumption of the biofilm (Fig. 4). At higher irradiance the upper part of the biofilm became supersaturated with respect to O_2 (reaching >5 times air saturation at an incident irradiance of 200 µmol photons·m^{-2}·s^{-1}), and the oxygen penetration depth increased to 2.0 mm (Figs. 3B, 4). The O_2 profiles changed immediately upon a change of the incident irradiance. It thus took <15–20 min of darkness to change the O_2 profile from the steady-state light situation shown in Figure 3B to the steady-state dark situation shown in Figure 3A.

The euphotic zone of the biofilm was only 0.5–0.7 mm thick due to a strong attenuation of photon scalar irradiance in the cyanobacterial surface layer (Figs. 3B, 4). The scattering of light led to a local maximum of photon scalar irradiance in the upper 0.0–0.2 mm of the biofilm approaching 120% of the incident surface irradiance. Below this narrow zone, photon scalar irradiance was attenuated exponentially with depth until less than 5–10% of the incident surface irradiance remained at 0.7 mm depth, which defined the bottom of the euphotic zone (Fig. 3B). Near-infrared light (NIR) was not absorbed by the cyanobacteria, and it consequently exhibited a much lower attenuation with depth. The scalar irradiance of NIR light reached up to 200% of the incident irradiance in the upper biofilm layers (data not shown).

Areal gross photosynthesis of the biofilm, P_g, increased with increasing irradiance and reached full saturation only at the highest irradiance used in the experiment (Fig. 5). By modeling the P_g vs. E_0 light saturation curve with a hyperbolic tangent function (Jassby and Platt 1976), a maximum photosynthetic capacity of P_{max} = 0.89 nmol O_2·cm^{-2}·s^{-1} was estimated for the biofilm. The initial slope of the P_g vs. E_0 curve, α, was 0.008. Hence, the scalar irradiance at the onset of light saturation of total biofilm photosynthesis, I_k, could be determined as $I_k = P_{max}/\alpha$ = 110 µmol photons·m^{-2}·s^{-1}. However, this estimate is based on a P vs. I curve with only one measurement at the highest scalar irradiance (Fig. 5) and therefore subject to some uncertainty.

It should be noted that the $P_g - I$ curve (Fig. 5) uses the scalar irradiance at the biofilm surface as the light intensity parameter. The total biofilm photosynthesis is thus related to the maximum amount of photons available at the biofilm surface rather than the incident irradiance. We found that the scalar irradiance, E_0, was ca. 20% higher than the incident irradiance, E_d, at the biofilm surface (Fig. 3B). Consequently, the onset of light saturation calculated from the P_g vs. E_d curve was 20% less (I_k = 92 µmol photons·m^{-2}·s^{-1}) than the I_k value calculated from the P_g vs. E_0 curve.

Spectral light attenuation and the action spectrum of photosynthesis. The spectral attenuation of light between 400 and 700 nm was very high ($K_0 > 5$ mm^{-1}) at all wavelengths but with distinct attenuation peaks at the major absorption wavelengths for cyanobacterial photopigments (Fig. 6). Peaks corresponding to absorption of chlorophyll *a* (Chl *a*) (440 and 675 nm), phycoerythrin (545–570 nm), and phycocyanin (615–625 nm) were found as well as a broad absorption band of various carotenoids (450–550 nm). The action spectrum for photosynthesis likewise exhibited a typical cyanobacterial pattern (cf. Jørgensen et al. 1987, Ploug et al. 1993), with most efficient photosynthesis occurring at phycobilin and Chl *a*

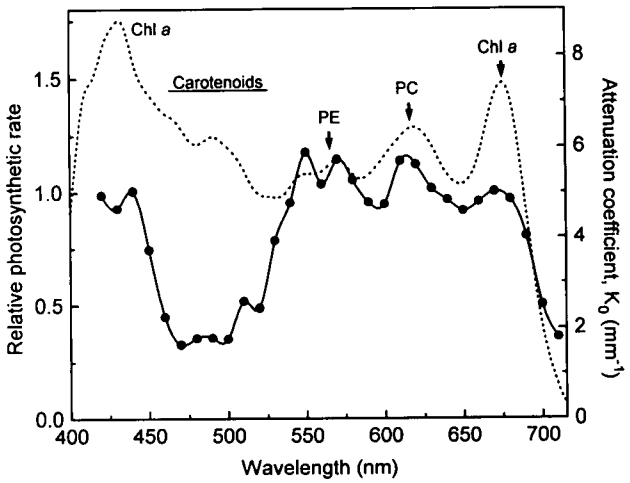

FIG. 6. Scalar irradiance attenuation spectrum (dotted curve) and action spectrum of photosynthesis in the upper 0.1 mm of a cyanobacterial biofilm (solid curve). The photosynthetic rates were normalized to the rate measured at 675 nm. Arrows indicate absorption wavelengths of Chl *a*, phycocyanin (PC), and phycoerythrin (PE).

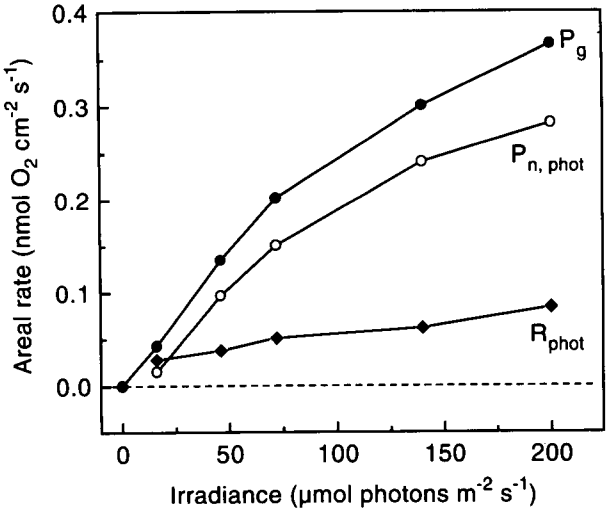

FIG. 7. Areal gross photosynthesis, P_g, net photosynthesis, $P_{n,phot}$, and O_2 respiration, R_{phot}, within the photic zone of a cyanobacterial biofilm at increasing incident photon irradiance.

absorption wavelengths (Fig. 6). The efficiency capability of light utilization for photosynthesis was low in the spectral range of carotenoid absorption although a high light attenuation was observed in the biofilm.

Photosynthesis-coupled respiration. From measured profiles of O_2 and photosynthesis, we calculated oxygen budgets for the biofilm in the dark and at an incident irradiance of 200 μmol photons·m^{-2}·s^{-1} (Fig. 3). The areal O_2 respiration in the dark, R_{dark}, was 0.073 nmol O_2·cm^{-2}·s^{-1}, whereas O_2 penetrated down to 0.5 mm. The average volumetric O_2 respiration in the dark was therefore 0.073/0.05 = 1.46 nmol O_2·cm^{-3}·s^{-1} (Fig. 3C). At an irradiance of 200 μmol photons·m^{-2}·s^{-1}, the areal oxygen respiration, $R_{light} = P_g - P_n$, was 0.57 nmol O_2·cm^{-2}·s^{-1} at a 2.0-mm O_2 penetration depth (Fig. 3B). Areal respiration of the illuminated biofilm was thus 7.8 times higher at an irradiance of 200 μmol photons·m^{-2}·s^{-1} than the areal dark respiration.

The areal O_2 respiration within the photic zone, $R_{phot} = P_g - P_{n,phot}$, was calculated to 0.30 nmol O_2·cm^{-2}·s^{-1}. The difference between these two numbers thus gives a total O_2 respiration in the nonphotosynthetic part of the illuminated biofilm of 0.27 nmol O_2·cm^{-2}·s^{-1}. The thickness of the photic zone was 0.65 mm, and the average volumetric O_2 respiration within the photic zone was therefore 0.30/0.065 = 4.6 nmol O_2·cm^{-3}·s^{-1}. The nonphotosynthetic aerobic part of the illuminated biofilm was 1.35 mm deep, which yields an average volumetric respiration below the photic zone of 2.0 nmol O_2·cm^{-3}·s^{-1} (Fig. 3C).

The O_2 budget of the photic zone as a function of irradiance was calculated in a similar experiment, where the surface of the biofilm was stabilized by a thin layer of agar (1% w/w) to reduce migration effects and to stabilize the DBL to facilitate accurate calculations of J_{up} (cf. Glud et al. 1992) (O_2 and photosynthesis profiles not shown). Both areal gross photosynthesis, P_g, and areal net photosynthesis of the photic zone, $P_{n,phot}$, increased with increasing irradiance (Fig. 7, Table 2). The areal O_2 respiration within the photic zone of the illuminated biofilm, R_{phot}, increased almost linearly from 0.028 nmol O_2·cm^{-2}·s^{-1} at low irradiance (16 μmol photons·m^{-2}·s^{-1}) to 0.084 nmol O_2·cm^{-2}·s^{-1} at high irradiance (200 μmol photons·m^{-2}·s^{-1}) (Fig. 7, Table 2). This increase was only partly due to an increasing thickness of the photic zone with increasing irradiance. The average volumetric O_2 respiration within the photic zone thus also increased from 0.67 nmol O_2·cm^{-3}·s^{-1} at low light to 1.08 nmol O_2·cm^{-3}·s^{-1} at high light (Table 2).

Effect of flow on photosynthesis and respiration. A control experiment showed that it was possible to induce reversible changes of the O_2 profile in experiments where the flow velocity was varied from one value to another and back again (Table 3). With increasing flow velocities, the DBL thickness decreased from >1 mm during stagnant conditions to <0.2 mm at the highest flow velocity (Fig. 8A–C). The decreasing DBL thickness resulted in steeper gradients across the DBL and, hence, in a more efficient diffusive solute exchange between biofilm and the overlying water at increasing flow velocities (Fig. 8A–C). The O_2 flux out of the illuminated biofilm, that is, the net photosynthesis, increased with flow velocity and was twice as high at a flow velocity of 10 cm·s^{-1} than under stagnant conditions (Table 3). However, the gross photosynthetic rate of the biofilm was largely unaffected by flow velocity. The O_2 concentration within the biofilm thus decreased with

TABLE 2. *Effect of incident irradiance on depth-integrated gross photosynthesis, P_g, and oxygen consumption in the photic zone. Depth profiles of oxygen and photosynthesis (data not shown) were measured as a function of incident irradiance while keeping temperature (20°C) and flow velocity (5 cm·s^{-1}) constant.*

Areal rates (nmol O_2·cm^{-2}·s^{-1})	Incident irradiance, E_d (400–700 nm) (μmol photons·m^{-2}·s^{-1})				
	16	46	72	140	200
Photosynthesis, P_g	0.043	0.135	0.202	0.301	0.366
Total oxygen export, $P_{n,phot}$	0.015	0.097	0.151	0.241	0.282
Photic zone respiration, R_{phot} (% of P_g)	0.028	0.038	0.051	0.062	0.084
Depth of photic zone (cm)	0.042	0.048	0.056	0.060	0.078
Specific respiration within photic zone (nmol O_2·cm^{-3}·s^{-1})	0.67	0.79	0.91	0.98	1.08

increasing flow velocity, and less of the produced O_2 was respired within the biofilm (Fig. 8, Table 3). The downward flux of O_2 to the nonphotosynthetic part of the biofilm consequently decreased with flow velocity, and the ratio of upward to downward O_2 flux changed from ca. 0.6 under stagnant conditions to 1.5 at a flow velocity of 10 cm·s^{-1} (Table 3).

At flow velocities at or above 14 cm·s^{-1}, the DBL was eroded away by turbulent eddies in the overlaying waterflow (Fig. 8D), and the transport of O_2 from the biofilm to the water was no longer dependent on molecular diffusion. The efficient advective transport of O_2 to the overlaying water therefore resulted in an O_2 concentration profile without oxygen supersaturation in the biofilm.

DISCUSSION

Optical properties of biofilms. The optical properties of biofilms and other light-scattering biological systems like sediments, plant, and animal tissue are fundamentally different from the optics of pelagic marine and freshwater systems (Wilson and Jaques 1990, Vogelmann et al. 1991, Kühl and Jørgensen 1994). The dense matrix of exopolymers and cell material make photosynthetic biofilms a complex heterogeneous optical system (Losee and Wetzel 1983). A major difference from pelagic systems is the importance of scattered light for photosynthetic organisms in such systems (Kühl and Jørgensen 1992b, Kühl et al. 1994b). Multiple scattering leads to a diffuse light field and to a local increase in photon pathlength per vertical distance traversed within the biofilm, thereby increasing the probability of absorption. The combination of scattering and a high density of absorbing photopigments leads to a strong light attenuation in the biofilm (Fig. 3B). The scalar irradiance attenuation coefficients found in this study (Fig. 6) are among the highest found in microbenthic communities (see e.g. Ploug et al. 1993 and Kühl et al. 1994b) and are 1000–10,000-fold higher than attenuation coefficients found in eutrophic lakes and in coastal waters (Kirk 1994). The volumetric gross photosynthesis of the biofilm also is 1000–10,000-fold higher than in most pelagic communities (Kirk 1994). The light attenuation and photosynthetic activity within 1 mm of biofilm is thus comparable in magnitude to the activities within a 10-m water column in pelagic systems.

Close to the surface of biofilms, that is, within the upper few hundred micrometers, a prolonged residence time of scattered photons caused by the local pathlength increase, combined with the continuous supply of incident photons from the light source, leads to a local maximum in photon flux density. If the refractive index of the biofilm is higher than that of the surrounding water, this local maximum in scalar irradiance would be further enhanced by a light-trapping mechanism due to total reflection of diffuse backscattered light at the biofilm–water interface (Wilson and Jaques 1990, Kühl and Jørgensen 1994). As a consequence of both the increase in local pathlength and the possible light trapping, a higher total quantum flux than the incident downwelling quantum flux is available for the photosyn-

TABLE 3. *Effect of flow velocity on depth-integrated gross photosynthesis, P_g, and oxygen respiration. Calculations were made on two experiments. In experiment I, oxygen and photosynthesis profiles were measured while the flow velocity was varied from 5 to 0 cm·s^{-1} and back to 5 cm·s^{-1} (data not shown). In experiment II, oxygen and photosynthesis was measured at a flow velocity of 0, 5, and 10 cm·s^{-1}, respectively (data shown in Fig. 8).*

Areal rates (nmol O_2·cm^{-2}·s^{-1})	Flow velocity (cm·s^{-1})					
	Experiment I			Experiment II		
	5	0	5	0	5	10
Photosynthesis, P_g	0.314	0.296	0.319	0.195	0.196	0.208
Upward O_2 flux, $J_{up} = P_n$	0.172	0.072	0.176	0.043	0.063	0.084
Respiration, R (% of P_g)	0.142 (45%)	0.224 (76%)	0.143 (45%)	0.152 (78%)	0.133 (68%)	0.124 (60%)
Downward O_2 flux, J_{down}	0.088	0.146	0.086	0.068	0.058	0.055
Ratio, J_{up}/J_{down}	1.950	0.490	2.050	0.630	1.090	1.530
Total oxygen export, $P_{n,phot}$	0.260	0.217	0.262	0.111	0.121	0.139
Photic zone respiration, R_{phot} (% of P_g)	0.054 (17%)	0.079 (27%)	0.057 (18%)	0.084 (43%)	0.075 (38%)	0.069 (33%)

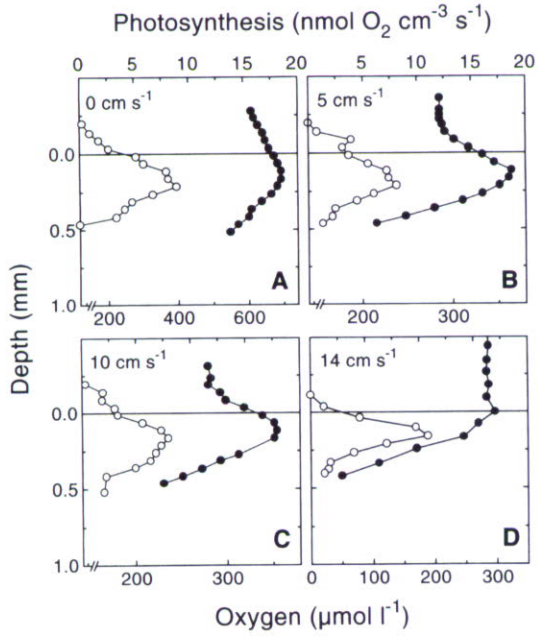

FIG. 8. O_2 concentration (●) and gross photosynthesis (○) depth profiles in a cyanobacterial biofilm at increasing flow velocity (indicated by numbers on graphs). A–C) Results measured in the same biofilm incubated at an incident irradiance of 80 µmol photons·m^{-2}·s^{-1}. D) Results from a different biofilm incubated at an irradiance of 70 µmol photons·m^{-2}·s^{-1}. Note different scales of O_2 concentration.

thetic microorganisms at the biofilm surface (Fig. 3B).

The magnitude of the scalar irradiance maximum varied with wavelength. Highest maxima were found at spectral wavelengths outside the absorption regions of major photopigments, especially in the NIR part of the spectrum. NIR light is scattered in the upper parts of sediments and biofilms and due to the low absorption NIR light penetrates efficiently into deeper layers of biofilms and sediments, where it can be used by bacteriochlorophyll-containing phototrophic bacteria (Kühl et al. 1994a). In this study we found no distinct spectral features of the NIR spectrum in the deeper layers of the biofilm, thus indicating the absence of a significant population of bacteriochlorophyll-containing bacteria.

A methodological consequence of the observed characteristics of the light field in biofilms is the need to relate photosynthesis measurements to actual scalar irradiance instead of to incident irradiance when the regulation of photosynthesis is investigated at the level of the microorganisms—for example, by microsensor measurements. Thus, both P vs. I curves and action spectra exhibit significant differences when light intensity is quantified as scalar irradiance instead of as incident irradiance (Jørgensen et al. 1987, Kühl et al. 1995). A comparison of microscale irradiance and scalar irradiance measurements in sandy sediments demonstrated that the actual light intensity available for the photosynthetic microorganisms could be underestimated by almost 100% by only measuring light intensity as incident irradiance (Kühl et al. 1994a). However, in most biofilms and sediments exhibiting a high density of phototrophs, the discrepancy between scalar irradiance and irradiance will be less due to a higher absorption to scattering ratio. It is our experience that in the visible part of the spectrum the scalar irradiance typically reaches ca. 110–160% of the incident irradiance at the surface of most photosynthetic biofilms and sediments.

While the availability of light for cells in the upper layers of the biofilm is enhanced by scattering, the effect on the total photosynthetic community may be the opposite, as scattering also enhances the probability for absorption with depth. In a study of light penetration in sand of different particle size an inverse relationship was thus found between the magnitude of scattering, that is, the surface maximum of scalar irradiance, and the depth of the photic zone (Kühl et al. 1994a). A more detailed account of the optics of microbenthic communities is given elsewhere (Kühl and Jørgensen 1994).

Light regulation of biofilm photosynthesis. Gross photosynthesis as measured with the oxygen microelectrode depends on the density of photosynthetic cells around the microsensor tip. Photosynthetic rates measured at various depths in the biofilm were consequently affected by any migration of the cyanobacteria at higher irradiances. When P vs. I curves were plotted for different depths, we observed a sharp decrease in photosynthesis in the surface layer and a distinct increase of photosynthesis in deeper layers of the photic zone at high irradiances (data not shown). It was not possible to discriminate whether photoinhibitory effects, migratory effects, or both were responsible for these changes in photosynthetic rates at specific points in the mat, and we did not attempt to further analyze P vs. I curves at different depths in the mat.

The areal gross photosynthesis of the biofilm exhibited only partial saturation with increasing irradiance due to a progressive stimulation of photosynthesis in deeper layers. The calculated onset of light saturation, I_k, of biofilm photosynthesis was 110 µmol photons·m^{-2}·s^{-1}, and the O_2 compensation point, that is, the irradiance above which the biofilm changed from a net heterotrophic to an autotrophic system, was already reached at an irradiance of 17.5 µmol photons·m^{-2}·s^{-1} (Fig. 4). These observations indicate a high photosynthetic efficiency of the cyanobacterial biofilm at low irradiances. A high photosynthetic efficiency is often found in benthic communities dominated by cyanobacteria (e.g. Revsbech et al. 1983, 1988, Lassen et al. 1992b, Epping and Jørgensen 1995). Recent studies of benthic cyanobacterial mats and pure cultures showed photosynthesis saturation even at low scalar irradiances ranging from 20 to 60 µmol photons·m^{-2}·s^{-1} (Ploug et al., unpubl., Prufert-Bebout,

unpubl.). In a study of P vs. I curves measured in various periphyton communities, Boston and Hill (1991) found I_k values ranging from 100 to 400 μmol photons·m^{-2}·s^{-1}. I_k values of 100–200 μmol photons·m^{-2}·s^{-1} and light compensation points of 20–40 μmol photons·m^{-2}·s^{-1} were found in epiphytic biofilms (Sand-Jensen et al. 1985, Sand-Jensen and Revsbech 1987).

Despite an efficient light utilization of the cyanobacteria, we found a scalar irradiance of ca. 15–25 μmol photons·m^{-2}·s^{-1} at the lower boundary of the euphotic zone in the biofilm (Figs. 3, 4), where photosynthesis was below the detection limit of the light–dark shift method. We cannot rule out a minor photosynthetic O_2 production below 0.5–0.7 mm, which was masked by a high O_2 consumption. But the absence of detectable photosynthesis may also indicate that parameters other than irradiance alone may limit photosynthesis at increasing depth in the biofilm. The lower boundary of the photic zone found in this study could be due either to direct growth limitation of the cyanobacteria or to an active avoidance (via migration) of deeper biofilm layers because of, for example, reduced light quality, nutrient limitations, or presence of toxic compounds like sulfide. The role of light quality for photosynthesis in benthic cyanobacterial communities was investigated by Ploug et al. (1993), who found that light intensity and gradients of chemical parameters probably play a more important role for photosynthesis regulation than the spectral shift in light quality due to self-shading at increasing depth in sediments and biofilms. Boston and Hill (1991) found that photosynthesis regulation of periphyton communities was correlated to biomass and parameters that regulate growth other than light intensity.

In the spectral regions of Chl *a* and phycobilin absorption, a good correspondance was found between attenuation spectra and action spectra for photosynthesis (Fig. 6). The action spectrum shows relatively low amounts of photosynthetically active carotenoids despite the high attenuation of 450–550-nm light (Fig. 6). This indicates that the carotenoids in the biofilm may primarily have a photoprotective role (Krinsky 1978). Photoprotective carotenoids are often found in cyanobacteria exposed to high irradiances (Palmisano et al. 1989, Oren et al. 1995), and low photosynthetic activity due to carotenoid absorption has also been found in other studies of action spectra in cyanobacterial mats and sediments (Jørgensen et al. 1987, Ploug et al. 1993, Ploug et al., unpubl. data).

Migration. Migration is an important adaptation for microorganisms to life in dynamic gradient environments such as biofilms, where dramatic changes of physical and chemical parameters occur over distances <0.1 mm and within time periods of a few minutes (Garcia-Pichel et al. 1994). We found a distinct horizontal migration pattern of the cyanobacteria at high irradiances, where the filaments formed dense tufts on the biofilm surface. A similar response to light was observed for the cyanobacterium *Oscillatoria terebriformis* in a hot spring microbial mat (Castenholz 1968, Richardson and Castenholz 1987). We did not observe any significant vertical migration into deeper biofilm layers at high light intensities. Vertical migration of cyanobacteria as a function of light intensity is frequently observed in microbial mats (Garcia-Pichel et al. 1994, Kühl et al. 1994b, Bebout and Garcia-Pichel 1995). However, high sulfide levels found in the deeper layers of the biofilm (cf. Kühl and Jørgensen 1992a, Ramsing et al. 1993) and/or the very dense and cohesive structure of the biofilm matrix may have prevented any significant downward migration.

In some experiments, changes in biofilm surface structure due to migration were minimized by covering the biofilm surface with a 1–1.5-mm-thin layer of agar (Glud et al. 1992, Fig. 7, Table 2). Control experiments showed no long-term inhibitory effect on the photosynthetic activity and on the O_2 profiles measured in the biofilm after addition of agar (Glud et al. 1992). The total photosynthetic rates measured in agar-covered biofilms were, however, lower than corresponding rates measured at the same irradiance in uncovered biofilms. Lower photosynthetic rates in the agar-covered biofilm could be due to a significant increase of the DBL thickness, which reduces the exchange rate of solutes (e.g. inorganic carbon) between the biofilm and overlaying water. The higher photosynthetic rates commonly observed in the uncovered biofilm could, however, also be due to the migration of the cyanobacteria.

More studies are needed to address the regulation of the observed migration behavior. Nondestructive techniques that allow monitoring of migratory behavior in biofilms at fine scale still need to be developed. One promising technique is based on measurements of reflectance spectra with fiber-optic microprobes to measure the fine scale distribution of specific groups of microalgae and photosynthetic bacteria (Kühl et al. 1994b, Bebout and Garcia-Pichel 1995).

DBL compression and diffusion geometry. The DBL thickness is reduced by the presence of a microsensor above the biofilm (Glud et al. 1994). This compression effect can lead to a higher solute exchange rate across the DBL and affects gradients within the biofilm. Such an effect may be of importance by changing the O_2/CO_2 ratio in the biofilm, especially if biofilm photosynthesis is dependent on the dissolved inorganic carbon (DIC) supply from the overlaying water. The effect of DBL compression on net and gross photosynthetic rates measured in photosynthetic microbial mats due to the presence of an O_2 microelectrode was investigated by Lorenzen et al. (1995). The main conclusions of their study were as follows: 1) the DBL compression effect was only detectable over smooth surface layers and was not found when the surface was irregular due to tufts

and formation of gas bubbles, 2) gross photosynthesis measured by O_2 microelectrodes was unaffected by the DBL compression, and 3) the total O_2 flux out of the photosynthetic layer was unchanged by the DBL compression, because a higher efflux through the compressed DBL was counterbalanced by a reduced downward flux into the O_2-consuming part of the mat. The DBL compression due to the presence of a microelectrode and its effects on the microgradients in photosynthetic communities is thus very similar to the effects of a DBL compression induced by an increased flow velocity in the overlaying water. We did not attempt to correct for a DBL compression in our data.

In thin artificially grown biofilms, a combined use of microsensors and laser confocal microscopy showed that such biofilms must be regarded as relative loose three-dimensional aggregations of cell clusters consisting of a mixture of very dense structures, where diffusional transport dominates, and of less dense structures and even open channels, where convective transport can take place (de Beer et al. 1994a, b). Obviously, the analysis of such a system in terms of one-dimensional diffusion geometry can result in serious misinterpretation. Furthermore, measuring photosynthesis with the light–dark shift technique in regions where advective transport is present (e.g. in porous biofilms and sediments) might cause problems with the method (Carlton and Wetzel 1987, Berninger and Hüttel, unpubl., Dodds unpubl. results). Further investigations of such effects are necessary to find the limits of the light–dark shift technique for photosynthesis measurements in the presence of advective transport processes.

The microstructure of the thick biofilm used in our study generally was very cohesive and dense (Fig. 1). Furthermore, the relatively low horizontal heterogeneity found in the investigated biofilm areas when numerous oxygen profiles were measured also indicated that the biofilm areas investigated could be modeled as a relatively flat and homogenous system, where diffusion was the dominant transport mechanism.

Light-enhanced respiration. We found a significant stimulation of respiration in illuminated biofilms as compared to dark-incubated biofilms. Total areal O_2 respiration of the biofilm when illuminated with 200 μmol photons$\cdot m^{-2}\cdot s^{-1}$ was almost 8 times higher than the dark respiration of the biofilm (Fig. 3C). Part of the enhanced areal O_2 respiration was due to a deeper oxygen penetration in the light as compared to the oxygen penetration in dark-incubated biofilms (Fig. 3A, B). The volumetric oxygen respiration was, however, also stimulated by light and was >3 times higher in the photic zone than the volumetric O_2 respiration in the dark (Fig. 3C). The light-enhanced respiration increased with irradiance, thus indicating a close coupling between photosynthesis and respiration (Table 2, Fig. 7), so that a significant part of the produced O_2 was respired internally in the biofilm. Similar patterns of light-enhanced respiration have been observed in biofilms (Kuenen et al. 1986, Jensen and Revsbech 1989), sediments (Revsbech et al. 1981, Lindeboom et al. 1985), microbial mats (Epping and Jørgensen 1995), and in the tissue of stony corals (Kühl et al. 1995). In the following we discuss possible explanations of light-enhanced respiration.

The DBL limited the O_2 flux to the biofilm in the dark, thereby controlling the areal dark respiration (Fig. 3A, Kühl and Jørgensen 1992a). In the light the DBL limited the transport of O_2 out of the biofilm and potentially the influx of, for example, DIC from the surrounding water to the biofilm. This can lead to O_2 supersaturation (Figs. 3B, 4, 8A–C), an increase of pH due to CO_2 fixation, and thus an increased O_2/CO_2 ratio within the photic zone. In illuminated biofilms, DIC limitation of photosynthesis might therefore occur and conditions favorable for photorespiration, that is, the O_2 consumption induced by the oxygenase activity of ribulose-1,5-bisphosphate carboxylase oxygenase (Raven and Beardall 1981), may develop.

If significant DIC limitation of biofilm photosynthesis was induced under stagnant or slow flow conditions due to a high O_2/DIC ratio, we would expect higher rates of gross photosynthesis at increasing flow velocities due to the more efficient supply of DIC (see e.g. Dodds 1989a). We did not observe any significant change in the gross photosynthetic rates with flow velocity (Fig. 8, Table 3), so we infer that the internal DIC pool of the biofilm due to respiratory processes in the biofilm was probably sufficient to avoid significant DIC limitation in the light. The irradiance used in the flow experiment was moderate (80 μmol photons$\cdot m^{-2}\cdot s^{-1}$), and we cannot rule out a possible DIC limitation at significantly higher irradiance. However, even at high irradiance, a significant part of the produced oxygen was consumed within the biofilm, both within and below the photic zone (Fig. 3C, Table 2). The high heterotrophic activity might thus have partly alleviated DIC limitation and photorespiration in the illuminated biofilms. Furthermore, cyanobacteria can use both CO_2 and HCO_3^- (converted to CO_2 by the enzyme carbonic anhydrase) in photosynthetic carbon fixation and have very low K_m values for photosynthetic CO_2 uptake as well as very efficient DIC uptake mechanisms (Aizawa and Miyachi 1986, Pierce and Omata 1988, Badger and Price 1992). Cyanobacteria may thus be well adapted to environments with high O_2/CO_2 ratios, such as microbenthic environments, and photorespiration is often regarded as a less important process in cyanobacteria.

In an earlier study, we investigated the role of photorespiration in the cyanobacterial biofilm by measuring photosynthesis and respiration in illuminated biofilms under various O_2/CO_2 ratios in the overlaying water and concluded that photorespiration was very low (Glud et al. 1992). We can

therefore probably rule out photorespiration as a major reason for the observed light-enhanced respiration. However, in biofilms dominated by diatoms (Glud et al. 1992) or composed of a mixture of green algae and cyanobacteria (Kuenen et al. 1986) indications for significant photorespiration were found. Furthermore, experiments in diatom biofilms indicated a pronounced DIC limitation of photosynthesis as a significant increase of gross photosynthesis and a concomitant decrease of respiration was observed at increasing flow velocity of the overlaying water (Glud et al., unpubl.).

The light-enhanced respiration we found in the cyanobacterial biofilm thus seems to be due to a direct stimulation of the heterotrophic processes by photosynthesis. In the light, O_2 was produced internally in the biofilm and thus alleviated the diffusion limitation for O_2 imposed by the DBL and O_2 penetrated 4 times deeper into the illuminated biofilm than in dark-incubated biofilms (Figs. 3, 4). The total zone of O_2 respiration was thus extended, and the areal respiration increased. Furthermore, both within and below the photic zone of the biofilm an increased volumetric respiration activity was found (Fig. 3C, Table 2). The affinity for O_2 is generally high in most heterotrophs, and low K_m values of <1–3 $\mu mol \cdot L^{-1}$ are reported in the literature (e.g. Hao et al. 1983). A stimulation of the volumetric O_2 respiration by enhanced O_2 availability is therefore unlikely.

Cyanobacteria excrete photosynthates, that is, simple organic compounds, in the light (Tolbert and Zill 1956, Fogg 1966, McFeters et al. 1978) that may fuel heterotrophic processes (Bauld and Brock 1974, Haack and McFeters 1982, Ward et al. 1987, Neely 1994). The biofilms were incubated in normal tap water without any additional organic carbon source, and heterotrophic processes were therefore mainly fueled by internal dissolved organic carbon sources, which might have limited respiration in the dark. We found a close microstructural association between the cyanobacteria and other bacteria in the biofilm (Fig. 1), and a direct stimulation of heterotrophic processes in the vicinity of the cyanobacteria by excretion of easily degradeable photosynthates could thus explain the enhanced volumetric respiration in the light. Such a metabolic coupling between autotrophic and heterotrophic processes was also recently infered from detailed biogeochemical studies of hypersaline microbial mats (Canfield and Des Marais 1993) and by Neely and Wetzel (1995), who found a strong positive correlation between bacterial and autotrophic productivity in periphyton and demonstrated a direct coupling of bacterial production to photosynthesis metabolism of microalgae and cyanobacteria in artificially grown biofilms.

Measures of primary productivity in biofilms. We have used several ways of expressing photosynthetic production in the biofilm. The areal net photosynthesis, P_n, measured as the flux of O_2 out of the biofilm to the overlaying water across the DBL is, in principle, comparable to the parameter measured in traditional gas exchange measurements. This parameter is sensitive to changes in DBL thickness due to, for example, changes in surface roughness due to migration or due to different flow velocities of the water. We thus showed a significant increase of P_n with increasing flow velocity, whereas the gross photosynthesis, P_g, was virtually unchanged (Fig. 8, Table 3). The total flux of O_2 out of the photic zone, $P_{n,phot}$, was much less affected by flow as the increase in the upward O_2 flux was partly compensated by a decrease of the downward O_2 flux at increasing flow velocity (Table 3).

Furthermore, P_n only expresses a part of the net carbon fixed (including excretion products as exopolymers), which becomes available for heterotrophic processes in the biofilm. A significant part of the produced O_2 and probably also a significant part of the fixed carbon was recycled internally in the biofilm due to the close association of cyanobacteria and heterotrophic bacteria. It thus seems that net photosynthesis calculated as the total flux out of the photic zone, $P_{n,phot}$, is a more reasonable measure of net primary productivity in microbenthic communities. Primary productivity in terms of O_2 production or DIC fixation is, however, a problematic term to define in biofilms and other communities where autotrophic processes are closely associated with, and may be fueled directly by, heterotrophic processes (Ludden et al. 1985, Jensen and Revsbech 1989).

Traditionally, areal respiration has been considered constant and equal to dark respiration in O_2 exchange studies of aquatic primary productivity (reviewed by Geider and Osborne 1992). Gross photosynthesis was then calculated as the sum of dark respiration and net photosynthesis measured by O_2 exchange in flux chambers. Our results in the cyanobacterial biofilm as well as other investigations of photosynthesis and respiration in sediments and microbial mats (Lindeboom et al. 1985, Epping and Jørgensen 1995) have shown that respiration is stimulated in the light and that the gas exchange method therefore underestimates gross photosynthesis significantly.

We present here fine-scale point measurements of O_2, light, photosynthesis, and respiration in biofilms using a one-dimensional diffusion-reaction model. Our aim was to demonstrate fundamental principles of the microenvironmental control of photosynthesis and respiration. Natural biofilms are, however, three-dimensional structures with a distinct topography, and quantitative studies thus essentially require a three-dimensional approach (Jørgensen and Des Marais 1990). Whereas point measurements with microsensors in smooth biofilm areas without gas bubbles may allow reliable calculations of the local net photosynthesis, that is, diffusive O_2 flux to the overlaying water, an extrapolation of these measures to a larger heterogeneous biofilm area would,

for example, lead to a serious underestimate of net photosynthesis at high irradiances, where intense formation and release of O_2 bubbles takes place, or if the solute exchange is significantly affected by the presence of animals in the biofilm. An extrapolation from the kind of data presented here to the overall quantitative regulation of biofilm primary productivity can therefore not be done without combining numerous microsensor measurements with other techniques that quantify biofilm photosynthesis and respiration on a larger scale, such as using gas exchange measurements or isotope techniques (Revsbech et al. 1981, Lindeboom et al. 1985, Geider and Osborne 1992, Canfield and Des Marais 1993).

We thank Anni Sølling for skillful assistance with the SEM analysis of biofilms. Anni Glud, Lars Borregaard Pedersen, and Carsten Lassen are thanked for construction of oxygen microelectrodes and scalar irradiance microprobes. Eric Epping, Bo Barker Jørgensen, Walter K. Dodds, and an anonymous reviewer are thanked for constructive criticism and suggestions. Financial support was provided by the Danish Biotechnology Program, the Danish Natural Science Research Council, the Carlsberg Foundation (Denmark), and the Max Planck Society (Germany).

Aizawa, K. & Miyachi, S. 1986. Carbonic anhydrase and CO_2 concentrating mechanisms in microalgae and cyanobacteria. *FEMS Microbiol. Rev.* 39:215–33.

Badger, M. R. & Price, G. D. 1992. The CO_2 concentrating mechanism in cyanobacteria and microalgae. *Physiol. Plant.* 84:606–15.

Bauld, J. & Brock, T. D. 1974. Algal excretion and bacterial assimilation in hot spring algal mats. *J. Phycol.* 10:101–6.

Bebout, B. M. & Garcia-Pichel, F. 1995. UVB-induced vertical migration of cyanobacteria in a microbial mat. *Appl. Environ. Microbiol.* 61:4215–22.

de Beer, D., Stoodley, P. & Lewandowski, Z. 1994a. Liquid flow in heterogeneous biofilms. *Biotechnol. Bioeng.* 44:6636–41.

de Beer, D., Stoodley, P., Roe, F. & Lewandowski, Z. 1994b. Effects of biofilm structures on oxygen distribution and mass transport. *Biotechnol. Bioeng.* 43:1131–8.

Boston, H. L. & Hill, W. R. 1991. Photosynthesis–light relations of stream periphyton communities. *Limnol. Oceanogr.* 36:644–56.

Broecker, W. S. & Peng, T. H. 1974. Gas exchange rates between air and sea. *Tellus* 26:21–35.

Canfield, D. E. & Des Marais, D. J. 1993. Biogeochemical cycles of carbon, sulfur, and free oxygen in a microbial mat. *Geochim. Cosmochim. Acta* 57:3971–84.

Carlton, R. G. & Wetzel, R. G. 1987. Distributions and fates of oxygen in periphyton communities. *Can. J. Bot.* 65:1031–7.

Castenholz, R. W. 1968. The behaviour of *Oscillatoria terebriformis* in hot springs. *J. Phycol.* 4:132–9.

Dalsgaard, T. & Revsbech, N. P. 1992. Regulating factors of denitrification in trickling filter biofilms as measured with the oxygen/nitrous oxide microsensor. *FEMS Microbiol. Ecol.* 101:151–64.

Dodds, W. K. 1989a. Microscale vertical profiles of N_2 fixation, photosynthesis, O_2, chlorophyll *a*, and light in a cyanobacterial assemblage. *Appl. Environ. Microbiol.* 55:882–6.

——— 1989b. Photosynthesis of two morphologies of *Nostoc parmelioides* (Cyanobacteria) as related to current velocities and diffusion patterns. *J. Phycol.* 25:258–62.

——— 1992. A modified fiber-optic light microprobe to measure spherically integrated photosynthetic photon flux density: characterization of periphyton photosynthesis–irradiance patterns. *Limnol. Oceanogr.* 37:871–8.

Epping, H. G. & Jørgensen, B. B. 1995. Light enhanced areal oxygen respiration in benthic phototrophic communities. *Mar. Ecol. Progr. Ser.* (in press).

Fogg, G. E. 1966. The extracellular products of algae. *Oceanogr. Mar. Biol. Annu. Rev.* 4:195–212.

Garcia-Pichel, F., Mechling, M. & Castenholz, R. W. 1994. Diel migrations of microorganisms in a hypersaline microbial mat. *Appl. Environ. Microbiol.* 60:1500–11.

Geider, R. J. & Osborne, B. A. 1992. *Algal Photosynthesis: The Measurement of Algal Gas Exchange.* Chapman & Hall, New York, 256 pp.

Glud, R. N., Gundersen, J. K., Revsbech, N. P. & Jørgensen, B. B. 1994. Effects on the benthic diffusive boundary layer imposed by microelectrodes. *Limnol. Oceanogr.* 39:462–7.

Glud, R. N., Jensen, K. & Revsbech, N. P. 1995. Diffusivity in surficial sediments and benthic mats determined by use of a combined N_2O-O_2 microsensor. *Geochim. Cosmochim. Acta* 59: 231–7.

Glud, R. N., Ramsing, N. B. & Revsbech, N. P. 1992. Photosynthesis and photosynthesis-coupled respiration in natural biofilms measured by use of oxygen microsensors. *J. Phycol.* 28:51–60.

Haack, T. K. & McFeters, G. A. 1982. Microbial dynamics of an epilithic mat community in a high alpine stream. *Appl. Environ. Microbiol.* 43:702–7.

Hao, O. J., Richard, M. G. & Jenkins, D. 1983. The half saturation coefficient for dissolved oxygen: a dynamic method for its determination and its effect on dual species competition. *Biotechnol. Bioeng.* 25:403–16.

Jassby, A. D. & Platt, T. 1976. Mathematical formulation of the relationship between photosynthesis and light for phytoplankton. *Limnol. Oceanogr.* 21:540–7.

Jensen, J. & Revsbech, N. P. 1989. Photosynthesis and respiration of a diatom biofilm cultured in a new gradient growth chamber. *FEMS Microb. Ecol.* 62:29–38.

Jørgensen, B. B. 1994. Diffusion processes and boundary layers in microbial mats. *In* Stal, L. J. & Caumette, P. [Eds.] *Microbial Mats: Structure, Development and Environmental Significance,* NATO ASI Series G, Vol. 35. Springer, Berlin, pp. 243–53.

Jørgensen, B. B., Cohen, Y. & Des Marais, D. J. 1987. Photosynthetic action spectra and adaptation to spectral light distribution in a benthic cyanobacterial mat. *Appl. Environ. Microbiol.* 53:879–86.

Jørgensen, B. B. & Des Marais, D. J. 1988. Optical properties of benthic photosynthetic communities: fiber-optic studies of cyanobacterial mats. *Limnol. Oceanogr.* 33:99–113.

——— 1990. The diffusive boundary layer of sediments: oxygen microgradients over a microbial mat. *Limnol. Oceanogr.* 35: 1343–55.

Jørgensen, B. B. & Revsbech, N. P. 1985. Diffusive boundary layers and the oxygen uptake of sediments and detritus. *Limnol. Oceanogr.* 30:111–22.

Karsten, U. & Kühl, M. 1996. Die Mikrobenmatte, das kleinste Ökosystem der Welt. *Biol. Unserer Zeit.* 1:16–26.

Kirk, J. T. O. 1994. *Light and Photosynthesis in Aquatic Ecosystems,* 2nd ed. Cambridge University Press, Cambridge, 509 pp.

Krinsky, N. I. 1978. Non-photosynthetic functions of carotenoids. *Phil. Trans. R. Soc. Lond., Ser. B* 284:581–90.

Kuenen, J. G., Jørgensen, B. B. & Revsbech, N. P. 1986. Oxygen microprofiles of trickling filter biofilms. *Water Res.* 20:1589–98.

Kühl, M., Cohen, Y., Dalsgaard, T., Jørgensen, B. B. & Revsbech, N. P. 1995. Microenvironment and photosynthesis of zooxanthellae in scleractinian corals studied with microsensors for O_2, pH and light. *Mar. Ecol. Prog. Ser.* 117:159–72.

Kühl, M. & Jørgensen, B. B. 1992a. Microsensor measurements of sulfate reduction and sulfide oxidation in compact microbial communities of aerobic biofilms. *Appl. Environ. Microbiol.* 58:1164–74.

——— 1992b. Spectral light measurements in microbenthic phototrophic communities with a fiber-optic microprobe coupled to a sensitive diode array detector. *Limnol. Oceanogr.* 37:1813–23.

——— 1994. The light field of microbenthic communities: ra-

diance distribution and microscale optics of sandy coastal sediments. *Limnol. Oceanogr.* 39:1368–98.

Kühl, M., Lassen, C. & Jørgensen, B. B. 1994a. Light penetration and light intensity in sandy marine sediments measured with irradiance and scalar irradiance fiber-optic microprobes. *Mar. Ecol. Prog. Ser.* 105:139–48.

——— 1994b. Optical properties of microbial mats: light measurements with fiber-optic microprobes. *In* Stal, L. J. & Caumette, P. [Eds.] *Microbial Mats: Structure, Development and Environmental Significance,* NATO ASI Series G, Vol. 35. Springer, Berlin, pp. 149–67.

Lassen, C., Ploug, H. & Jørgensen, B. B. 1992a. A fibre-optic scalar irradiance microsensor: application for spectral light measurements in sediments. *FEMS Microbiol. Ecol.* 86:247–54.

——— 1992b. Microalgal photosynthesis and spectral irradiance in coastal marine sediments of Limfjorden, Denmark. *Limnol. Oceanogr.* 37:760–72.

Lindeboom, H. J., Sandee, A. J. J., & de Klerk-van den Driessche, H. A. J. 1985. A new bell jar/microelectrode method to measure changing oxygen fluxes in illuminated sediments with a microalgal cover. *Limnol. Oceanogr.* 30:693–8.

Lorenzen, J., Glud, R. N. & Revsbech, N. P. 1995. Impact of microsensor-caused changes in diffusive boundary layer thickness on O_2 profiles and photosynthetic rates in benthic communities of microorganisms. *Mar. Ecol. Prog. Ser.* 119: 237–41.

Losee, R. F. & Wetzel, R. G. 1983. Selective light attenuation by the periphyton complex. *In* Wetzel, R. G. [Ed.] *Periphyton of Freshwater Ecosystems.* Dr. W. Junk, The Hague, pp. 89–96.

Ludden, E., Admiraal, W. & Colijn, F. 1985. Cycling of carbon and oxygen in layers of marine microphytes; a simulation model and its eco-physiological implications. *Oecologia* 66: 50–9.

McFeters, G. A., Stuart, S. A. & Olson, S. B. 1978. Growth of heterotrophic bacteria and algal extracellular products in oligotrophic waters. *Appl. Environ. Microbiol.* 35:383–91.

Neely, R. K. 1994. Evidence for positive interactions between epiphytic algae and heterotrophic decomposers during decomposition of *Typha latifolia. Arch. Hydrobiol.* 129:443–57.

Neely, R. K. & Wetzel, R. G. 1995. Simultaneous use of 14C and 3H to determine autotrophic production and bacterial production in periphyton. *Microb. Ecol.* 30:227–37.

Nielsen, L. P., Christensen, P. B., Revsbech, N. P. & Sørensen, J. 1990. Denitrification and oxygen respiration in biofilms studied with a microsensor for nitrous oxide and oxygen. *Microb. Ecol.* 19:63–72.

Oren, A., Kühl, M. & Karsten, U. 1995. An endoevaporitic microbial mat within a gypsum crust: zonation of phototrophs, photopigments, and light penetration. *Mar. Ecol. Prog. Ser.* 128:151–9.

Paerl, H. W. & Shimp, S. L. 1973. Preparation of filtered plankton and detritus for study with scanning electron microscopy. *Limnol. Oceanogr.* 18:802–5.

Palmisano, A. C., Cronin, S. E., D'Amelio, E. D., Munoz, E. & Des Marais, D. J. 1989. Distribution and survival of lipophilic pigments in a laminated microbial mat community near Guerrero Negro, Mexico. *In* Cohen, Y. & Rosenberg, E. [Eds.] *Microbial Mats: Physiological Ecology of Benthic Microbial Communities.* American Society of Microbiology, pp. 138–52.

Pierce, J. & Omata, T. 1988. Uptake and utilization of inorganic carbon by cyanobacteria. *Photosynth. Res.* 16:141–54.

Ploug, H., Lassen, C. & Jørgensen, B. B. 1993. Action spectra of microalgal photosynthesis and depth distribution of spectral scalar irradiance in a coastal marine sediment of Limfjorden, Denmark. *FEMS Microbiol. Ecol.* 102:261–70.

Ramsing, N. B., Kühl, M. & Jørgensen, B. B. 1993. Distribution of sulfate-reducing bacteria, O_2, and H_2S in photosynthetic biofilms determined by oligonucleotide probes and microelectrodes. *Appl. Environ. Microbiol.* 59:3840–9.

Raven, J. A. & Beardall, J. 1981. Respiration and photorespiration. *In* Platt, T. [Ed.] *Physiological Bases and Phytoplankton Ecology. Can. Bull. Fish. Aquat. Sci.* 210:55–82.

Revsbech, N. P. 1989. An oxygen microelectrode with a guard cathode. *Limnol. Oceanogr.* 34:474–8.

Revsbech, N. P. & Jørgensen, B. B. 1983. Photosynthesis of benthic microflora measured by the oxygen microprofile method: capabilities and limitations of the method. *Limnol. Oceanogr.* 28:749–56.

Revsbech, N. P., Jørgensen, B. B., Blackburn, T. H. & Cohen, Y. 1983. Microelectrode studies of the photosynthesis and O_2, H_2S, and pH profiles of a microbial mat. *Limnol. Oceanogr.* 28:1062–74.

Revsbech, N. P., Jørgensen, B. B. & Brix, O. 1981. Primary production of microalgae in sediments measured by oxygen microprofile, $H^{14}CO_3^-$ fixation, and oxygen exchange methods. *Limnol. Oceanogr.* 26:717–30.

Revsbech, N. P., Nielsen, J. & Hansen, P. K. 1988. Benthic primary production and oxygen profiles. *In* Blackburn, T. H. & Sørensen, J. [Eds.] *Nitrogen Cycling in Coastal Marine Environments.* Wiley, New York, pp. 69–83.

Richardson, L. L. & Castenholz, R. W. 1987. Diel vertical movements of the cyanobacterium *Oscillatoria terebriformis* in a sulfide-rich hot spring microbial mat. *Appl. Environ. Microbiol.* 53:2142–50.

Sand-Jensen, K. & Revsbech, N. P. 1987. Photosynthesis and light adaptation in epiphyte–macrophyte associations measured by oxygen microelectrodes. *Limnol. Oceanogr.* 32:452–7.

Sand-Jensen, K., Revsbech, N. P. & Jørgensen, B. B. 1985. Microprofiles of oxygen in epiphyte communities on submerged macrophytes. *Mar. Biol. (Berl.)* 89:55–62.

Tolbert, N. E. & Zill, L. P. 1956. Excretion of glycolic acid by algae during photosynthesis. *J. Biol. Chem.* 222:895–906.

Vogelmann, T. C., Martin, G., Chen, G. & Buttry, D. 1991. Fibre optic microprobes and measurement of the light microenvironment within plant tissues. *Adv. Bot. Res.* 18:255–95.

Ward, D. M., Tayne, T. A., Anderson, K. L. & Bateson, M. M. 1987. Community structure and interactions among community members in hot spring cyanobacterial mats. *In* Fletcher, M., Gray, T. R. S. & Jones, J. G. [Eds.] *Ecology of Microbial Communities.* Cambridge University Press, Cambridge, pp. 179–210.

Williams, S. L. & Carpenter, R. C. 1990. Photosynthesis/photon flux density relationships among components of coral reef algal turfs. *J. Phycol.* 26:40–50.

Wilson, B. C. & Jaques, S. L. 1990. Optical reflectance and transmittance of tissues: principles and applications. *IEEE J. Quant. Electron.* 26:2186–99.